Journal of Physics: Conference Series

**PAPER** • **OPEN ACCESS**

# Isospin equilibration phenomenon and mid-rapidity IMF emission in the $^{48}Ca + ^{27}Al$ 40 MeV/nucleon collision

To cite this article: M Papa *et al* 2020 *J. Phys.: Conf. Ser.* **1643** 012103

# Isospin equilibration phenomenon and mid-rapidity IMF emission in the $^{48}Ca +^{27} Al$ 40 MeV/nucleon collision

**M Papa[1], L Acosta[2], G Cardella[1], E De Filippo[1], F Favela[2], E Geraci[3], B Gnoffo[4], G Lanzalone[5], C Maiolino[4], N S Martorana[4,3], A Pagano[1], E V Pagano[4], S Pirrone[1], G Politi[3], L Quattrocchi[6], F Rizzo[3], P Russotto[4], A Trifiro'[6] and M Trimarchi[6]**

[1] INFN, Sezione di Catania - Catania,Italy
[2] Universidad Nacional autonoma de Mexico- Mexico city, Mexico
[3] Universit'a degli studi di Catania Dip. di Fisica e Astronomia - Italy
[4] INFN Laboratori Nazionali del Sud - Catania, Italy
[5] Universit'a degli studi di Enna Kore - Enna,Italy
[6] Universit'a degli studi di Messina Dip. di scienze MIFT - Messina, Italy

E-mail: `Massimo.Papa@ct.infn.it`

**Abstract.** It is discussed the dynamics of Isospin equilibration in reactions involving the production of Intermediate Mass Fragment (IMF) in the mid-rapidity region. The investigation proceeds through the measurements of the reduced value of the total dipolar signal obtained from the measured velocities and charges of all fragments produced in the collision $^{48}Ca +^{27} Al$ at 40 MeV/nucleon. Preliminary experimental results, along with the comparison with CoMD-III model calculations for different density functionals related to the symmetry energy, are presented.

## 1. Introduction

Isospin equilibration phenomena have been studied, also in the recent past, by performing reactions at Fermi energies between nuclei having pronounced differences in the charge/mass ratio [1,2,3]. In this context, equilibration means the spontaneous tendency experienced by two colliding slabs of nuclear matter to re-distribute uniformily the neutron/proton ratio in the phase-space accessible to the investigated systems. Different model calculations (see [2,4]) relate this effect to the well-known diffusion-drift phenomena well established in the thermodynamics of non-equilibrated infinite (closed) systems. In the context of nuclear physics, the interest in this phenomenon is due to its connection with the symmetry energy associated with the iso-vectorial nuclear forces. In the past, these processes were investigated essentially in binary reactions, i.e. relatively fast processes, through the study of the charge-mass distribution of the fragments produced in the reaction. More recently, they have been also investigated through the determination of the asymptotic dipolar signal [5] arising from the strong correlation between velocities and multiplicity of the produced fragments in the dynamical stage. In the next section, we discuss briefly how this observable is related to the dynamics of the heavy-ion collision process. In Section 3 we illustrate results obtained on the reaction $^{48}Ca +^{27} Al$ at 40 MeV/nucleon concerning a preliminary analysis on events characterized by an Intermediate Mass Fragment (IMF) emission at mid rapidity. Finally, a section will be devoted to the final remarks.

## 2. Dipolar signals and the collision dynamics

In the Fermi energy domain, the heavy-ion collisions are interpreted phenomenologically through a fast pre-equilibrium stage described using dynamical models and a later-stage described by statistical decay models. The two stages involve rather different densities and excitation energies, being the dynamical stage able to populate the most exotic regions of Nuclear Matter (even if only for a short time). This will produce a kind of mixing effect in the value of the parameters governing the density functionals of the effective interaction that is the basic quantity in every model aiming to describe the collision process. Even if, for peripheral and semi-peripheral collisions, the angular correlations can help in disentangling statistical effects from dynamical ones [6,7], in multi-fragmentation or in more central processes the separation can be rather problematic. To better understand the need to separate the effects produced by the two reaction stages, we shortly recall the role played by the Isospin in the statistical decay processes. Statistical decay determines the final cooling mechanism of the hot sources already at an excitation energy of the primary sources of about 2-3.5 MeV/A; this heavily affects the charge/mass of the final products. In statistical models, the isospin affects the level density and the temperature producing remarkable effects on light charged particle multiplicity [8,9]. The multi-step statistical cascade (first step or last step) could affect also the isoscaling parameters. These parameters were widely used to describe the ratio between charge-mass distributions of fragments produced in collisions between similar systems [10]. All these dependencies can produce in many cases a blurring of the primary effects produced in the dynamical stage. With the aim of clearly disentangle the two stages described above, also in case of complex processes, we decided to investigate the following observable:

$$\langle \overrightarrow{D} \rangle = \langle \sum_{i=1}^{m} Z_i(\overrightarrow{V}_i - \overrightarrow{V}_{c.m.}) \rangle_{\mathcal{K}}. \quad (1)$$

$Z_i$ and $\overrightarrow{V}_i$ are respectively the charge and velocity of the generic particle produced in the collision. The brackets indicate the average over an ensemble $\mathcal{K}$ of selected events. $\overrightarrow{V}_{c.m}$ is the center of mass (c.m.) velocity and $m$ is, event by event, the number of charged fragments. The interest in this quantity is twofold:

a) as shown in [11], this quantity is closely linked with charge/mass equilibration process because it represents the average time derivative of the total dipolar signal in the asymptotic stage (expressed in unit of $e$). As shown from dynamical microscopic calculations, in a collision between two nuclei 1 and 2 having different charge/mass asymmetries, $\mid \langle \overrightarrow{D} \rangle \mid$ changes with time from the value: $\mid \langle \overrightarrow{D} \rangle \mid \equiv \mid \overrightarrow{D}_m \mid = \mid \frac{1}{2} \langle \mu \rangle (\langle \beta_2 \rangle - \langle \beta_1 \rangle)(\langle \overrightarrow{V}_1 - \overrightarrow{V}_2 \rangle) \mid$ to smaller values during the pre-equilibrium stage, thus reflecting the spontaneous approach to equilibrium.

b) because of the symmetries of the statistical decay mode, $\langle \overrightarrow{D} \rangle$ is not affected by the statistical emission of all sources produced in later stages. This essentially happens because due to the vectorial character of this quantity the statistical effects are self-averaged to zero [11] for well reconstructed events. Therefore, $\langle \overrightarrow{D} \rangle$ is a well suited global variable to selectively evidence dynamical effects related to the Isospin equilibration process. To better illustrate this,

in Figure 1 we show as a function of time the average dipolar signals and the density in the c.m. of the $^{48}Ca + ^{27}Al$ colliding system. The calculations are performed with the CoMD-III model [12,13]. We can see that the average dipolar signal reaches a constant value in a relatively short time (about 100 fm/c), though the statistical cooling mechanism of the hot sources goes on for a much longer time. From the density plot is also observed that the largest changes of the dipolar

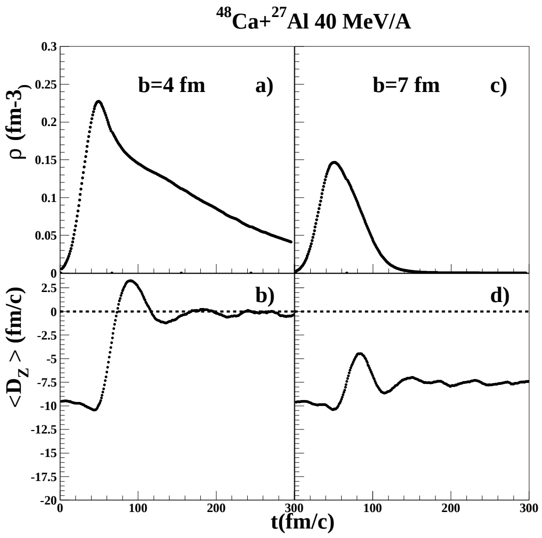


**Figure 1.** CoMD-III calculations for the $^{48}Ca +^{27} Al$ system. The dipolar signals and the c.m. average density are plotted as a function of time for two different impact parameters

signal is strongly correlated in time to the largest variation of the density as compared to the saturation value.

## 3. Experimental results on the $^{48}Ca +^{27} Al$ system at 40 MeV/A

The first experimental investigation [5] was the $^{48}Ca$+$^{27}Al$ reaction at 40 MeV/A with the multi-detector CHIMERA [14,15] at the LNS laboratories. In this first stage of the investigation, we measured the effective partial dipolar signal $\langle D^c_Z \rangle$ along the beam axis. The reduced value of the dipolar signal is obtained by replacing, event by event, the center of mass velocity, which appears in the definition of $\langle D_Z \rangle$, with the one related to the subsystem formed by all identified charged particles. In this way, possible systematic errors are eliminated. Good agreement with CoMD-III model calculations was obtained for different sizes of the projectile-like fragment, by using a value of potential symmetry energy at the saturation density $E_{p,sym}$ equal to 16 MeV and a related stiffness parameter $\gamma \simeq 0.8 - 1$ (see below). In this contribution we report on a new preliminary analysis performed on a different class of selected events associated with the production of an IMF ($Z > 2$) in the mid-rapidity region. As described above, the selected events are the ones for which it has been possible to properly reconstruct the total charge and momentum of the system after the collision. In Figure 2 and Figure 3 we display the experimental data and the preliminary CoMD-III calculations respectively, concerning the bi-dimensional plot $Z - V_{par}$ for all fragments produced in the selected events. It is possible to observe clearly that the mid-rapidity zone between the PLF and TLF velocities is highly populated. In the bottom panels, the plots represent events (Pro.IMF) for which the IMF velocity is located in the PLF region ($\overrightarrow{V}_{Z,i} > \overrightarrow{V}_{c.m.}$) while the central ones (Tar.IMF) are related to IMF with velocity in TLF region $\overrightarrow{V}_{Z,i} < \overrightarrow{V}_{c.m.}$ In the upper panels we display the total contribution (Mid.IMF).

From the figures we can see that the correlation $Z - V_{par}$ observed experimentally are qualitatively reproduced by the model. In Figure 4 the reduced values $\langle D^c_Z \rangle$ for the three sub-classes of events are reported in the upper 3 panels. The experimental results (black square) are compared with CoMD-III+GEMINI calculations (red dot points) performed using

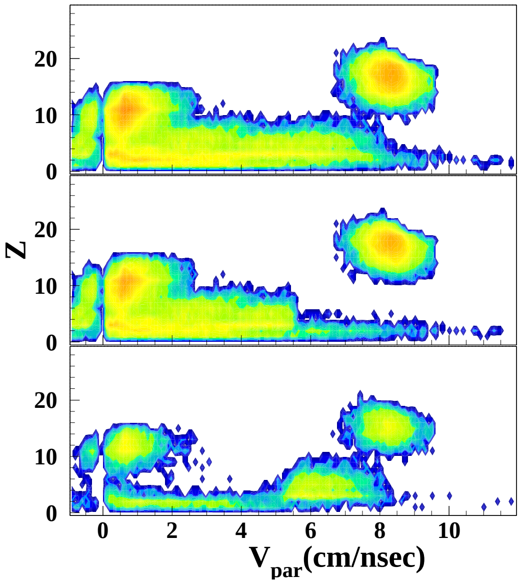


**Figure 2.** Experimental $Z - V_{par}$ plot for the class of selected events (see the text).

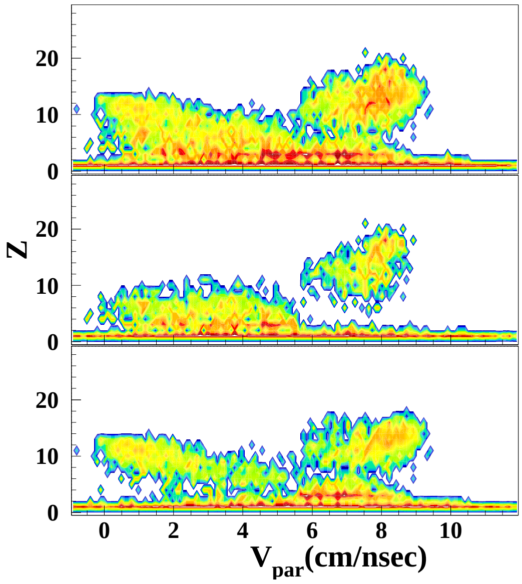


**Figure 3.** CoMD-III+GEMINI $Z - V_{par}$ for the analogue class of calculated events (see the text).

different stiffness values $\gamma$, describing the density dependence of the potential symmetry energy according to the following expression: $E_{p,sym}(\rho) = E_{p,sym}(\rho_0)(\frac{\rho}{\rho_0})^{\gamma}$ (in the limit of a mean field approach) with $E_{p,sym}(\rho_0)$=16 MeV . Finally, in the bottom panel for the three values of the $\gamma$ parameters, we plot the difference between the theoretical $\langle D_Z \rangle$ values and the reduced $\langle D_Z^c \rangle$. These differences can be interesting because they represent the global contribution of neutron emission to the isospin equilibration phenomenon [5]. Statistical errors associated to the mean values are within the size of the marked points. From Figure 4 we see that the best agreement for the reduced dipolar signal in Pro.IMF events is obtained with a pronounced soft symmetry energy $\gamma = 0.5$ while the one for Tar.IMF gives a slightly better agreement with the $\gamma = 1.$ case. Calculations show also an interesting feature concerning the balance between the number of Pro.IMF and Tar.IMF events. They show, in fact, a dependence on the $\gamma$ value. The yield of PLF splitting increases by decreasing the $\gamma$ value. Finally, the last panel shows an average negative contribution of the emitted neutrons to the equilibration process for Pro.IMF events and a positive one for Tar.IMF break-up. This behaviour can be related, trough simple considerations, to an average neutron velocity centred on the PLF side in the first case and on the TLF side in the second one. Finally, we observe that the absolute value of $\langle D_Z \rangle$ , for the global process and the partial ones, decreases with $\gamma$ indicating a larger degree of equilibration for softer iso-vectorial interaction.

## 4. Final remarks

The results that we have shown in this contribution show rather high sensitivity of the dipolar signal to the stiffness of the iso-vectorial forces. In this analysis the comparison with data concerning Pro.IMF shows a good agreement for $\gamma = 0.5$ while $\gamma \simeq 1$ describes better a kind of Tar.IMF disassembly. Even if the reaction mechanisms that we describe are rather different (also by considering the binary process discussed in [5]) and therefore involve probably

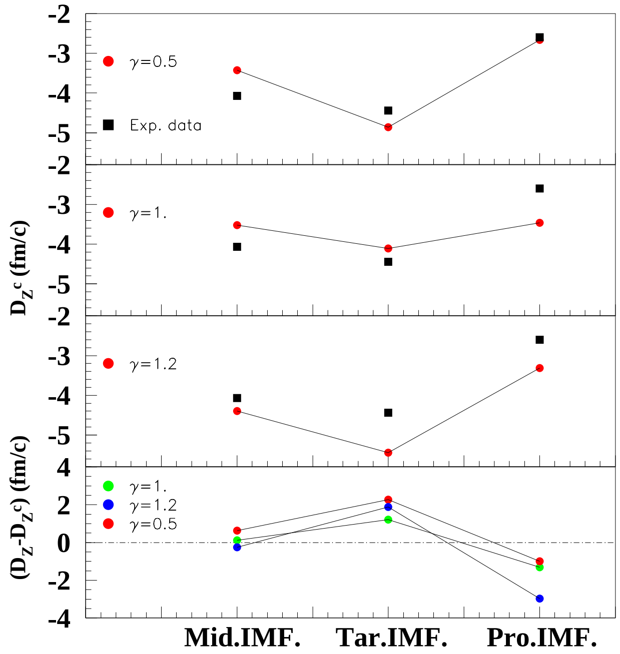


**Figure 4.** In the three upper panels, we show the comparison between CoMD-III+GEMINI results concerning the reduced value of the dipolar signals and the corresponding experimental values. Different panels correspond to different stiffness of the potential symmetry energy. In the bottom panel the differences of the total values and the reduced ones are also shown.

different dominant average densities, the global comparison point out pronounced differences in the stiffness parameter values. Nevertheless, we have to remark the preliminary character of this analysis, especially concerning the comparison with model calculations that surely need the introduction of an accurate description of the filtering effects related to the experimental apparatus. This further analysis should improve the comparison between the experimental $Z - V_{par}$ correlations and the calculated one in the target-like-fragment region (see Figures 2 and 3) and therefore also the global comparison concerning the dipolar signals.

## 5. References

[1] Tsang M B *et al* 2004 *Phys. Rev.* C **87** 024603
[2] Danielewicz P and Lee J 2014 *Nucl. Phys.* A **87** 1
[3] Brown K, Hudan S, deSouza J, Gautier J, Roy R, Shetty D V, Soliutis G A and Yennello S J 2014 *Phys. Rev.* C **87** 061601
[4] Li B, Chen L, Ko C *et al* 2008 *Phys. Rep.* **464** 113
[5] Papa M *et al* 2015 *Phys. Rev.* C **91** 041601R
[6] Russotto P *et al* 2015 *Phys. Rev.* C **91** 014610
[7] De Filippo E *et al* 2019 *IL NUOVO CIMENTO* C **42** 97
[8] Cussol D *et al* 2002 *Phys. Rev.* C **65** 044604
[9] Brondi D *et al* 2010 *EPJ Web of Conferences* 04002
[10] Zhou P, Tian W D , Ma Y G , Cai X Z , Fang D Q and Wang H W 2011 *Phys. Rev.* C 84 036705
[11] Papa M *et al* 2005 *Phys. Rev.* C **72** 064608.
[12] Papa M *et al* 2013 *Phys. Rev.* C **87** 014001
[13] Papa M, Maruyama T and Bonasera A*et al* 2001 *Phys. Rev.* C **62** 024612

[14] Cardella G *et al* 2016 *IL NUOVO CIMENTO* C **39** 407
[15] Pagano A *et al* 2012 *Nucl. Phys. News* **22** 25